Temperature and pressure-induced valence transitions in YbNi$_2$Ge$_2$ and YbPd$_2$Si$_2$

Hitoshi Yamaoka,[1] Ignace Jarrige,[2] Naohito Tsujii,[3] Jung-Fu Lin,[4] Nozomu Hiraoka,[5] Hirofumi Ishii,[5] and Ku-Ding Tsuei[5]

[1]*Harima Institute, The Institute of Physical and Chemical Research (RIKEN), Sayo, Hyogo 679-5148, Japan*
[2]*Synchrotron Radiation Research Unit, Japan Atomic Energy Agency, 1-1-1 Kouto, Sayo, Hyogo 679-5148, Japan*
[3]*Quantum Beam Center, National Institute for Materials Science, 1-2-1 Sengen, Tsukuba 305-0047, Japan*
[4]*Department of Geological Sciences, Jackson School of Geosciences, The University of Texas at Austin, Austin, Texas 78712, USA*
[5]*National Synchrotron Radiation Research Center, Hsinchu 30076, Taiwan*

We have measured the temperature and pressure-induced Yb valence transitions in tetragonal YbNi$_2$Ge$_2$ and YbPd$_2$Si$_2$ using x-ray absorption spectroscopy in the partial fluorescence yield mode and resonant x-ray emission spectroscopy. A temperature dependence of the Yb valence on the order of 0.1 has been measured, consistent with the magnetic-susceptibility study. The crossover from the low-temperature state having a stronger mixed valence to a high-temperature local moment behavior is analyzed within the Anderson impurity model. Pressure-induced second-order valence transitions are observed for both compounds with a more gradual transition in YbPd$_2$Si$_2$ than that of YbNi$_2$Ge$_2$. The mean valences are slightly less than 3+ at ambient pressure but increase with applying pressure. Small variations in the Yb valence on the order of 0.03–0.05 can result in drastic change in the physical properties such as magnetic order and transport properties. Our results show that the Yb valence is noninteger around the quantum critical point.

PACS number(s): 75.30.Mb, 71.20.Eh, 78.70.En, 78.70.Ck

I. INTRODUCTION

Heavy-fermion intermetallic compounds of rare-earth and actinide elements attract much attention due to their interesting physical properties, including superconductivity and strong exchange correlations. Particularly, ternary rare-earth compounds containing Ce, Eu, and Yb with a ThCr$_2$Si$_2$-type tetragonal structure[1] have been of great interest for a few decades. Among them, the RM_2X_2 (R122, where R=Ce, Yb, U, M=transition metal, X=Si, Ge) system is well known to exhibit heavy-fermion character whereas superconductivity was discovered in CeCu$_2$Si$_2$.[2] In these compounds, yet the transition metal is nonmagnetic but the magnetic properties result from the Ruderman-Kittle-Kasuya-Yoshida (RKKY) exchange interaction with the conduction electrons. The compounds with R=Y, La, and Lu are normally Pauli paramagnets, though the ones with R=Ce, Yb mixed valence and Kondo effect are favored because the energy difference between the trivalent and divalent valence states is small.[3] Accordingly, the physical properties of Ce122 and Yb122 and their temperature and pressure dependences have been the center of intense research attention.

Here we focus on two archetypal R122 compounds, YbNi$_2$Ge$_2$ and YbPd$_2$Si$_2$, with a tetragonal ThCr$_2$Si$_2$ crystal structure belonging to the space group $I4/mmm$. These compounds were shown to be in the mixed valence state by x-ray absorption spectroscopy.[4] The electric specific-heat coefficient (γ) $\sim$ 136 mJ/(mol K^2) for YbNi$_2$Ge$_2$ points to a heavy-fermion behavior.[5] The ratio of the A coefficient in the resistivity curve ($\rho = \rho_0 + AT^2$) to the γ does not follow the Kadowaki-Woods law,[6,7] indicating that the ground-state degeneracy of the total angular momentum J=7/2 is preserved. At ambient pressure the ground state of YbNi$_2$Ge$_2$ is Fermi liquid with a T^2 dependence of the resistivity while magnetic order occurs above the quantum critical point (QCP) at about 5 GPa.[8]

YbPd$_2$Si$_2$ shows a moderately large γ $\sim$ 203 mJ/(mol K^2).[9,10] Temperature dependence of the resistivity indicates a T^2 dependence at less than 25 K and thus the system is in the Fermi-liquid state at ambient pressure. No phase transition down to 45 mK was observed in the resistivity measurement and the QCP in the vicinity of 0–1 GPa has been suggested.[11] The effective magnetic moment μ_{eff}=4.5 $\pm$ 0.1 μ_B is larger than that of YbNi$_2$Ge$_2$,[12,13] but slightly smaller than that of Yb^{3+}. The crystal electric field (CEF) effect of YbPd$_2$Si$_2$ was extensively studied.[13–17] A recent high-pressure study of the thermoelectric and dilatometric properties disclosed a phase transition around 6 ± 0.5 GPa.[18] They discuss the possibility that a small valence fluctuation results in the phase transition, but neither direct measurement of the pressure dependence of the valence of YbPd$_2$Si$_2$ has been reported yet nor for YbNi$_2$Ge$_2$.

We here investigate the temperature and pressure effects on the electronic structure of YbPd$_2$Si$_2$ and YbNi$_2$Ge$_2$, using two complementary hard x-ray spectroscopies, partial fluorescence yield x-ray absorption spectroscopy (PFY-XAS) and resonant x-ray emission spectroscopy (RXES).[19–25] RXES yields truly bulk-sensitive information about the electronic structure. It is well suited to the study of subtle pressure-induced changes in the electronic state of rare-earth compounds.[26] External pressure is a clean, highly accurate way to tune the lattice parameter, hence the valence in the case of valence-fluctuating compounds, compared with chemical substitution which is not free from undesired structural disorder-related effects. A direct measurement of the valence as a function of pressure is therefore crucial to better understand the crossover phenomenon between the Kondo effect with mixed valence and the antiferromagnetic order at the QCP.[27–31] Our high-pressure data show that the valence gradually increases toward trivalency for both compounds and provide evidence for the valence state to be still noninteger around the QCP for YbNi$_2$Ge$_2$. We discuss the temperature dependence of the experimentally derived valence

in the light of numerical results based on the Anderson impurity model.[32–34]

II. EXPERIMENTS

Single-crystalline samples of $YbNi_2Ge_2$ were prepared by an in-flux method similar to Ref. [5]. For $YbPd_2Si_2$, we used polycrystalline samples, which were made by argon arc melting and subsequent annealing. The magnetic susceptibility was measured with a superconducting quantum interference device magnetometer at an applied field of 1000 Oe.

PFY-XAS and RXES measurements were performed at the Taiwan beamline BL12XU, SPring-8. The undulator beam was monochromatized by a pair of Si(111) crystals and focused to a size of 20 (horizontal) $\times$ 50 (vertical) μm^2 at the sample position using a combination of toroidal and K-B mirrors. The incident photon flux was estimated to be about 8×10^{12} photons/s at 8.9 keV as measured by a pin diode (type S3590-09). A Johann-type spectrometer equipped with a spherically bent Si(620) crystal (radius of ~ 1 m) was used to analyze the Yb $L\alpha_1(3d_{5/2} \rightarrow 2p_{3/2})$ emission line with a solid-state detector (XFlash 1001 type 1201). The overall energy resolution was estimated to be about 1 eV around the emitted photon energy of 7400 eV from the elastic scattering. The intensities of all spectra are normalized by the incident-beam intensity monitored just before the target. A closed-circuit He cryostat was used for the low-temperature measurements. The samples were subjected to high pressure using a diamond anvil cell with a Be-gasket and silicone oil as the pressure transmitting medium. The pressure was estimated from the ruby fluorescence shift.

III. RESULTS AND ANALYSES

A. Magnetic susceptibility

The temperature dependence of the magnetic susceptibility χ of $YbNi_2Ge_2$ and $YbPd_2Si_2$ is shown in Fig. 1. In Fig. 1(b) in order to ensure a reliable measurement, we present two sets of susceptibility data for $YbPd_2Si_2$: one was collected on a powder randomly oriented sample solidified by paraffin oil to avoid the magnetic anisotropy effect, and the other one was measured on a field-oriented sample prepared by melting the powder sample in the paraffin oil and cooling under a magnetic field of 5 T. The data for $YbPd_2Si_2$ taken from Ref. [13] are also shown. The difference of the susceptibility between the randomly oriented and field-oriented samples are due to the effect of the magnetocrystalline anisotropy, also resulting the difference of the Weiss temperature as will be described below. According to the Bethe-Ansatz solution of the Coqblin-Schrieffer model, the physical properties of a Kondo lattice are scaled by a single energy parameter (T_0).[32–34] We estimate the characteristic temperatures (corresponding to the Kondo temperature) by using Rajan's numerical results.[33] We fit the Rajan's curves (Rajan's fit) to the experimental result of the magnetic susceptibility, leaving T_0 as a fitting parameter for $\nu = 4(J = 3/2)$ and $8(J = 7/2)$, where $\nu (\nu = 2J + 1)$ and J are the ground-state degeneracy and total angular momentum, respectively. In these fits we used the relation to drive the
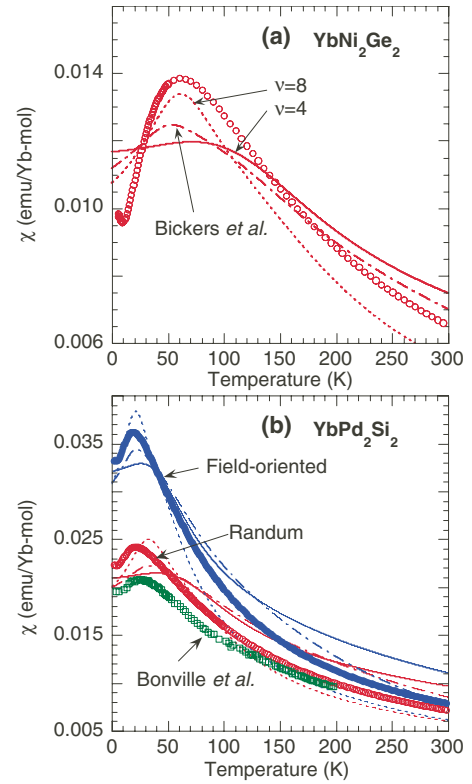

FIG. 1. (Color online) Temperature dependence of the magnetic susceptibility (χ) of (a) $YbNi_2Ge_2$ and (b) $YbPd_2Si_2$. In (b) two kinds of susceptibility data (the solidified powder sample and the sample without solidification under the magnetic field of 5 T) are shown. The solid and dashed lines represent the fit based on Rajan's calculations (Ref. [33]) for a degeneracy of $\nu=4$ (solid lines) and 8 (dashed lines), respectively. A dashed-dotted line is based on the calculation by Bickers *et al.* (Ref. [34]) The data for $YbPd_2Si_2$ taken from Fig. 4 in Ref. [13] are also shown in (b).

susceptibility at $T=0$ limit: $\chi(0)T_0 = N_A \nu(\nu - 1)g_L^2 \mu_B^2/(24\pi k_B)$, where N_A is the Avogadro's number, ν the ground-state degeneracy, g_L the Landé factor, μ_B the Bohr magnetron, and k_B the Boltzmann constant. It is noted that in both compounds the ground state is in the intermediate valence state and the Kondo limit $(n_f=1)$, which is assumed in the Rajan's calculations, is not valid. Thus we also analyzed the susceptibility based on the calculations by Bickers *et al.*[34] (Bickers' fit) as shown in Fig. 1. The fit, however, yields almost the same characteristic temperature of $T_0=222$ K with that of Rajan's fit (220 K), due to the fact that n_f is nearly 1 at the intermediate temperature limit. In $YbPd_2Si_2$ the Rajan's fits with $\nu=8$, $\nu=4$, the and Bickers' fit result the characteristic temperatures ranging 139 K, 136 K, and 142 K for the field-oriented sample and 90 K, 89 K, and 92 K for the randomly oriented sample, respectively. It is known that the CEF effect lifts the degeneracy in $YbPd_2Si_2$.[10,13,17] The CEF for Yb^{3+} is on the order of 100 K and thus physical properties of the Kondo lattice having $T_0 \sim 87$ K (Ref. [10]) such as $YbPd_2Si_2$ is a result of the competition between the CEF interaction and c-f hybridization,[35] and the characteristic temperatures for randomly oriented sample, obtained from the fits to our measured data, are com-

TABLE I. Physical parameters of $YbNi_2Ge_2$ and $YbPd_2Si_2$. The lattice parameters, Weiss temperature (Θ_p), Curie constant (C), magnetic moment (μ), specific-heat coefficient (γ), A coefficient in the resistivity curve ($\rho=\rho_0+AT^2$), Kodowaki-Woods parameter (A/γ^2), and Wilson ration (R_W).

| | Lattice | | | | | | | | |
	a (Å)	c (Å)	Θ_p (K)	C (emu K/mol)	μ (μ_B)	γ (mJ/mol K^2)	A ($\mu\Omega$ cm/K^2)	A/γ^2 ($\mu\Omega$ cm mol^2 K^2/mJ^2)	R_W
$YbNi_2Ge_2$	4.001[a]	9.733[a]	-88	2.54	4.50	136[b]	0.00776[a]	4.2×10^{-7}	1.2[c]
$YbPd_2Si_2$	4.093[d]	9.872[d]	-59,[e] -29 [f]	2.59,[e] 2.61[f]	4.50[d]	203[d]	0.356[g]	8.6×10^{-6}	0.3

[a]Reference 8.
[b]Reference 5.
[c]Reference 42.
[d]Reference 13.
[e]Field-oriented sample.
[f]Randomly oriented sample.
[g]From the fit to the data in Ref. 47.

parable to this value. In $YbNi_2Ge_2$ T_0 is higher than 100 K therefore the CEF may be less effective.

We also made a Curie-Weiss fit to the high-temperature susceptibility. The Curie-Weiss-type paramagnetic susceptibility χ is described as: $\chi=C/(T-\Theta_p)+$const, where C and Θ_p are the Curie constant and Weiss temperature, respectively. The Curie constant is written as $C=N_A\mu^2/3k_B$ with μ being the effective magnetic moment. In the valence fluctuating Yb systems, the effective magnetic moment can be used as a measure of the degree of valence admixture, since the Yb^{3+} ion has a magnetic moment of 4.54 μ_B while Yb^{2+} is nonmagnetic. That is, the inverse susceptibility should be a linear function of T as $1/\chi=T/C-\Theta_p/C$ at temperatures high enough where both Kondo and CEF effects are less important. Thus we estimated the effective magnetic moment and the Weiss temperature and effective magnetic moment from the slope of the linear part of $1/\chi(150<T<300$ K). The results are summarized in Table I with other parameters. In $YbNi_2Ge_2$ the effective magnetic moment reported to be $\mu_{eff}=3.51$ μ_B by Oesterreicher and Parker[36] seems to be too small. The derived Weiss temperatures are -88 K for $YbNi_2Ge_2$ and -59 K (field-oriented sample) and -29 K (randomly oriented sample) for $YbPd_2Si_2$, suggesting them having the mixed valence states.

B. Temperature dependence

Figure 2 summarizes the temperature dependence of the Yb L_3 PFY-XAS spectra and Yb $2p_{3/2}3d_{5/2}$-RXES spectra collected at the maximum of the Yb^{2+} resonance (incident photon energy $E_{in}=8934$ eV) for $YbNi_2Ge_2$ and $YbPd_2Si_2$. The RXES spectra are plotted as a function of the energy transfer, which is defined as the difference between the incident and emitted photon energies. It is noted that the intensity of Yb^{2+} in the PFY-XAS spectra is relatively small compared to that of Yb^{3+}. The Yb^{2+} component is, however, resonantly enhanced at $E_{in}=8934$ eV and thus we can observe the changes in the intensity clearly for both Yb^{2+} and Yb^{3+} components in the RXES spectra. The intensity of both RXES and PFY-XAS spectra is normalized by the area of the fluorescence spectrum measured at $E_{in}=8970$ eV. Insets in

Figs. 2(a) and 2(b) correspond to the enlarged PFY-XAS Yb^{2+} peak. Although the main component is Yb^{3+}, these spectra clearly show evidence of the valence fluctuation in both systems. For both compounds, as the temperature were decreased, the intensity of the Yb^{2+} component increased while that of Yb^{3+} decreased, pointing to an enhancement of the valence fluctuations. We estimate the Yb valence through the curve-fitting procedure detailed in Refs. 19–24 and the results are shown in Fig. 3. We briefly describe the fitting procedure of the PFY-XAS spectra. After subtracting an arctangentlike (asymmetrical double sigmoid) function corresponding to the continuum excitations, two Voigt functions are used to fit the $f^1(Yb^{3+})$ component centered at 8946 eV and the $f^2(Yb^{2+})$ contribution around 8934 eV, respectively. For the fit of the RXES spectra, we use two Voigt functions for the $f^1(E_{tr}\simeq=1522$ eV) and $f^2(E_{tr}\simeq=1528$ eV) components, respectively, where E_{tr} is the energy transfer.

In the Anderson impurity model (AIM) the temperature dependence of the valence follows the equation: $v(T)=2+n_f(\infty)-[\Delta n_f(T)/\Delta n_f(0)]\Delta n_f(0)$, where $n_f(\infty)$ and $\Delta n_f(T)$ are the intermediate temperature limit of the valence and the total decrease in valence, respectively.[24,34] $\Delta n_f(T)/\Delta n_f(0)$ was calculated as a function of T/T_0. We fit the data, leaving $n_f(\infty)$ and $\Delta n_f(0)$ as free parameters.[37] The results of the fit are shown in Fig. 3(a) for $YbNi_2Ge_2$ and Fig. 3(c) for $YbPd_2Si_2$, using T_0 estimated from the fit to the magnetic susceptibility in Fig. 1. The temperature dependence of the valence for $YbPd_2Si_2$ is well described by the AIM while that of $YbNi_2Ge_2$ is not quite satisfactory. The discrepancy can be explained by the higher Kondo temperature of $YbNi_2Ge_2$ compared to $YbPd_2Si_2$, resulting in a temperature dependence of the valence that stretches above room temperature for $YbNi_2Ge_2$, whereas the valence is observed to already saturate near room temperature in the case of $YbPd_2Si_2$ [cf. Fig. 3(c)]. Measuring the valence through the whole temperature range of the mixed-valence regime, up to the valence saturation near trivalence, appears therefore to be a necessary ingredient to a successful fit. Another possibility is that the AIM is not applicable to $YbNi_2Ge_2$, and that we should instead use the Anderson lattice model, which usually shows a slower crossover from a low-temperature state hav-
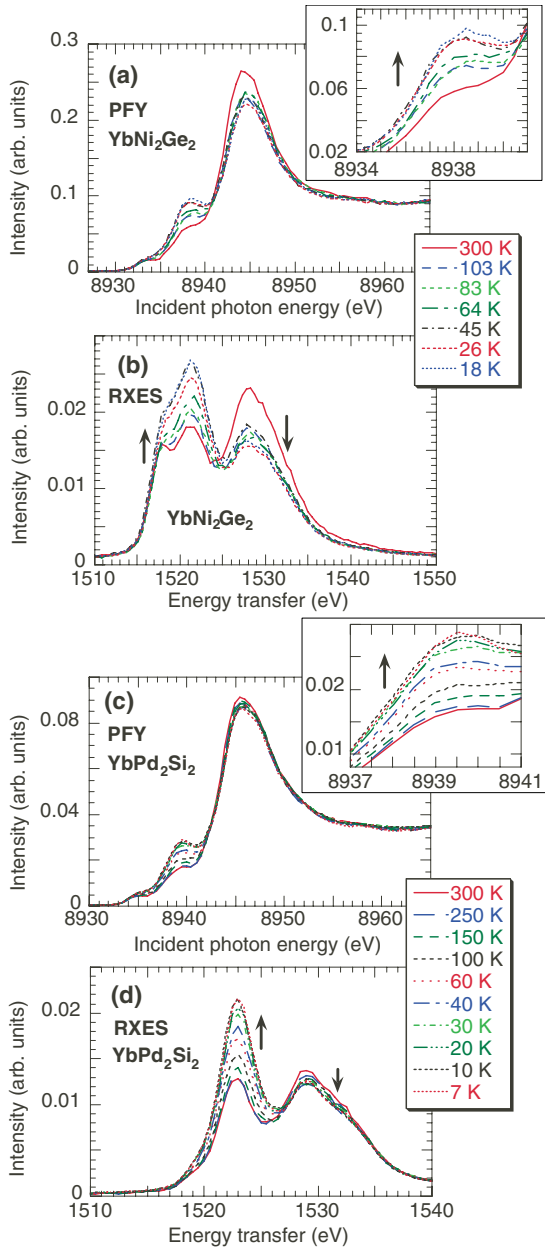
FIG. 2. (Color online) Temperature dependence of the Yb L_3 PFY-XAS and Yb $3d_{5/2}2p_{3/2}$-RXES (E_{in}=8934 eV) spectra measured from YbNi$_2$Ge$_2$ and YbPd$_2$Si$_2$. The inset in each figure represents the enlarged 2+ component and the arrows indicate the trend of the intensity with decreasing temperature.

ing a higher mixed valence to a high-temperature local-moment behavior.[38] This means that the screening of the local moment upon cooling is significantly protracted and that one may need to consider two energy scales, the Kondo temperature and the coherent temperature, to account for the physics of YbNi$_2$Ge$_2$.[39,40]

In Fig. 3(c) a fit when with T_0 as free parameter is also shown and the T_0 is estimated to be about 68 K. As can be seen in Fig. 3(c) both curves for T_0=90 and 68 K agree with the experimental result within the error bars. The temperature dependence of valence in YbPd$_2$Si$_2$ has been roughly measured by Sampathkumaran *et al.*[12] using conventional
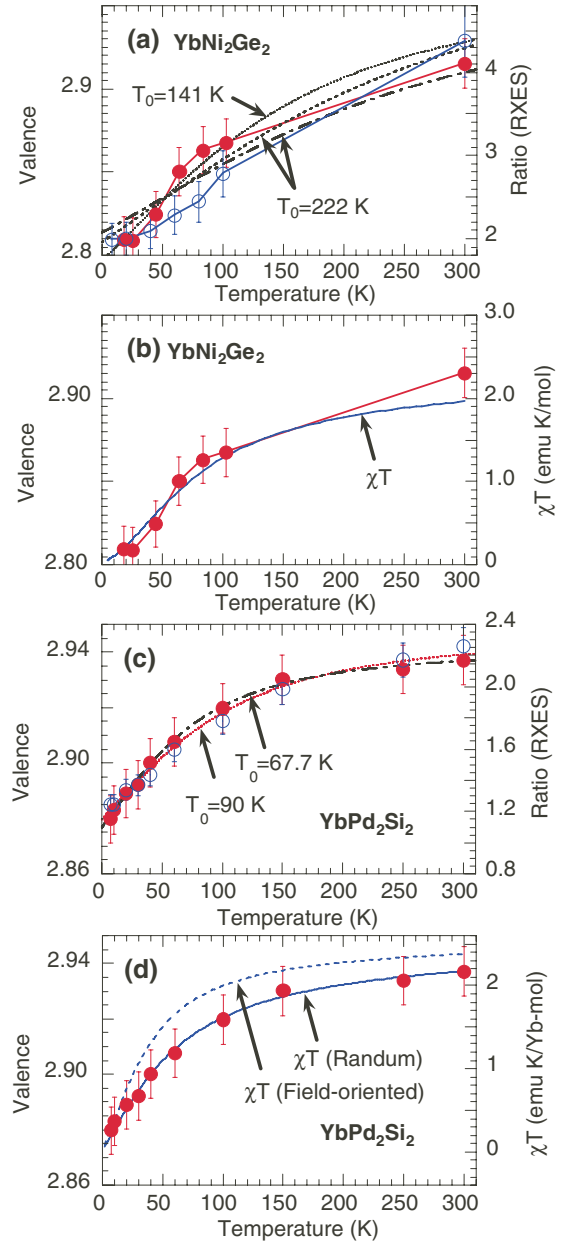

FIG. 3. (Color online) Temperature dependence of the Yb valence (closed circles) derived from the PFY-XAS spectra. Open circles correspond to the intensity ratio of Yb^{2+} to Yb^{3+} derived from the RXES spectra at E_{in}=8934 eV. In (a) a dotted, a broken and a dashed-dotted lines correspond to the AIM calculations for D=1 eV and T_0=141 K (fit parameter), D=1 eV and T_0=222 K, and n_f=0.988 (fit parameter) and T_0=222 K, respectively. In (c) a dotted and a dashed-dotted lines corresponds to AIM calculations for n_f=0.948 (fit parameter) and T_0=90 K (given parameter), and n_f=0.948 (fit parameter) and T_0=67.7 K (fit parameter), respectively. The temperature dependence of χT is also shown along with the valence in (b) and (d).

XAS and analyzed by Schlottmann,[10] but the accuracy of our PFY-XAS (and RXES, cf. Sec. III C) data is higher, ensuring a more reliable analysis. Derived values of $n_f(\infty)$ and $\Delta n_f(T)$ are summarized in Table II along with the c-f hybridization energy (Γ) and the D, where $\Delta n_f(0)=1/[1+\nu\Gamma/(\pi T_0)]$.[34] In Table II estimated physical parameters are summarized with

TABLE II. Derived and input parameters in the model calculations in Figs. 1 and 3. T_m, $T_0(T_K)$, T_{coh}, and T_{sf} correspond to maximum temperature of the temperature dependence of the resistivity, characteristic temperature (Kondo temperature), coherent temperature where Fermi-liquid behavior is observable, and spin fluctuation temperature, respectively. The characteristic temperature T_0 is the derived values from the AIM fit for magnetic susceptibility in Fig. 1. $n_f(\infty)$, Δn_f, Γ, and D are intermediate temperature limit of the valence, total decrease in valence, c-f hybridization energy, and conduction-electron bandwidth, respectively (Ref. 34).

	T_m (K)	$T_K(T_0)$ (K)	T_{coh} (K)	T_{sf} (K)	$n_f(\infty)$	$\Delta n_f(0)$	Γ (meV)	D (eV)	ν
YbNi$_2$Ge$_2$	50	222		80[a]	0.988	0.354	14	67	8
		222			0.963	0.292	14	1	
		141			0.963	0.326	10	1	
YbPd$_2$Si$_2$	30[b]	~90	25[c]	58[d]	0.948	0.133	44	0.74	4

[a]Reference 42.
[b]Reference 12.
[c]Reference 47.
[d]Reference 41.

other parameters taken from the literatures. The spin-fluctuation temperature for YbPd$_2$Si$_2$ is included too,[41] but this value seems not to be reliable because of the CEF effect. In practice T_{sf} is comparable to the Kondo temperature and the saturation of the $\chi T/T$ curve as a function of T/T_{sf} occurs around 0.75, suggesting the CEF effect.[42] In Table II the value of the c-f hybridization energy Γ for YbPd$_2$Si$_2$ is comparable to that estimated by Bonville *et al.*[13] For YbNe$_2$Ge$_2$ a physically unreasonable value of D is obtained, due to the overestimated value of $n_f(\infty)$ that stems from the too narrow temperature range of our measurement on the high-temperature side (cf. paragraph above). Therefore inversely we assumed a physically reasonable value of $D=1$ eV,[43] derived $n_f(\infty)$, and made two kinds of fits: one using T_0 $=222$ K as a given value and the other leaving T_0 as a free parameter. As shown in Fig. 3(a), better fits are obtained in the case of $D=1$ eV. In Figs. 3(b) and 3(d), it is observed that an excellent agreement between the valence and χT is obtained for both compounds, similarly to the YbInCu$_4$-based compounds.[23] The decrease in χT with temperature simply corresponds to the decrease in the magnetic Yb^{3+} component, Yb^{2+} being nonmagnetic.

C. RXES

The RXES spectra measured on YbNi$_2$Ge$_2$ at 300 K and 18 K and YbPd$_2$Si$_2$ at 300 K as a function of the incident energy across the Yb L_3 edge are shown in Fig. 4. The vertical offset of the RXES spectra in the top panels of Fig. 4 is scaled to the incident energy axis of the PFY-XAS spectra. The contour plots of the RXES spectra are shown in the middle panels. Going from low to high incident photon energy, one can successively observe the Raman regime where the peaks remain at constant energy transfer, progressively evolving into the fluorescence which shifts toward high transfer energies. Each spectrum is fitted with three components corresponding to the Raman 2+ and 3+ and the fluorescence and the results are shown in lower panels. These results also indicate the decrease in the valence with decreasing temperature. The valences are estimated to be v $=2.86\pm0.03$ at 18 K and $v=2.95\pm0.03$ at 300 K for

YbNi$_2$Ge$_2$, and $v=2.94\pm0.03$ at 300 K for YbPd$_2$Si$_2$. The values of the valence shown in Fig. 3(b) were estimated from the PFY-XAS analysis. The difference between the values estimated by PFY-XAS and RXES can usually be ascribed to the uncertainty of the PFY-XAS analysis due to the overlap of the $2p\rightarrow5d$ peaks with the arctanlike part corresponding to the excitations toward the continuum. We note that although this uncertainty may slightly affect the absolute value of the valence, the estimation of the relative changes as a function of temperature or pressure remains accurate.[24]

Groshev *et al.*[44] derived a value of $v=2.74\pm0.04$ for YbNi$_2$Ge$_2$ by using the line shift of the K x rays, but this value seems to be too small based on our results. For YbPd$_2$Si$_2$, Sampathkumaran *et al.*[12] obtained $v=2.82\pm0.08$ at 16 K and $v=2.89\pm0.08$ at 300 K from the analysis of their XAS spectra. Besnus *et al.*[45] derived $v=2.89$ from the specific-heat measurement. Schlottmann[10] analyzed the magnetic susceptibility of YbPd$_2$Si$_2$ by the Anderson model with $\nu=4$ and $T_K=87$ K and obtained $v=2.82$ at $T=0$ K. These values are overall comparable to our estimations based on RXES.

D. Pressure dependence

Figure 5 shows the pressure dependence of the Yb L_3 PFY-XAS and Yb $2p3d$-RXES spectra measured for YbNi$_2$Ge$_2$ and YbPd$_2$Si$_2$. Analyzed results are shown in Figs. 6(a) and 6(c). The intensity ratio of Yb^{2+} to Yb^{3+} in the Yb RXES spectra measured at $E_{in}=8934$ eV is also shown. In Fig. 6(b) the values of A and the magnetic-ordering temperature T_m are also plotted.[8] For both compounds the valence gradually increases with increasing pressure and approaches trivalence where the magnetic character is likely to become dominant. We note that in Yb compounds such small change in the valence induces drastic changes in the physical properties although the valence is already near 3+ at ambient pressure.

A high-pressure study of the electrical resistivity of YbNi$_2$Ge$_2$ suggested the existence of a QCP around 4 GPa, corresponding to a transition from a Fermi liquid to a magnetically ordered state.[8] The pressure dependence of T_I,
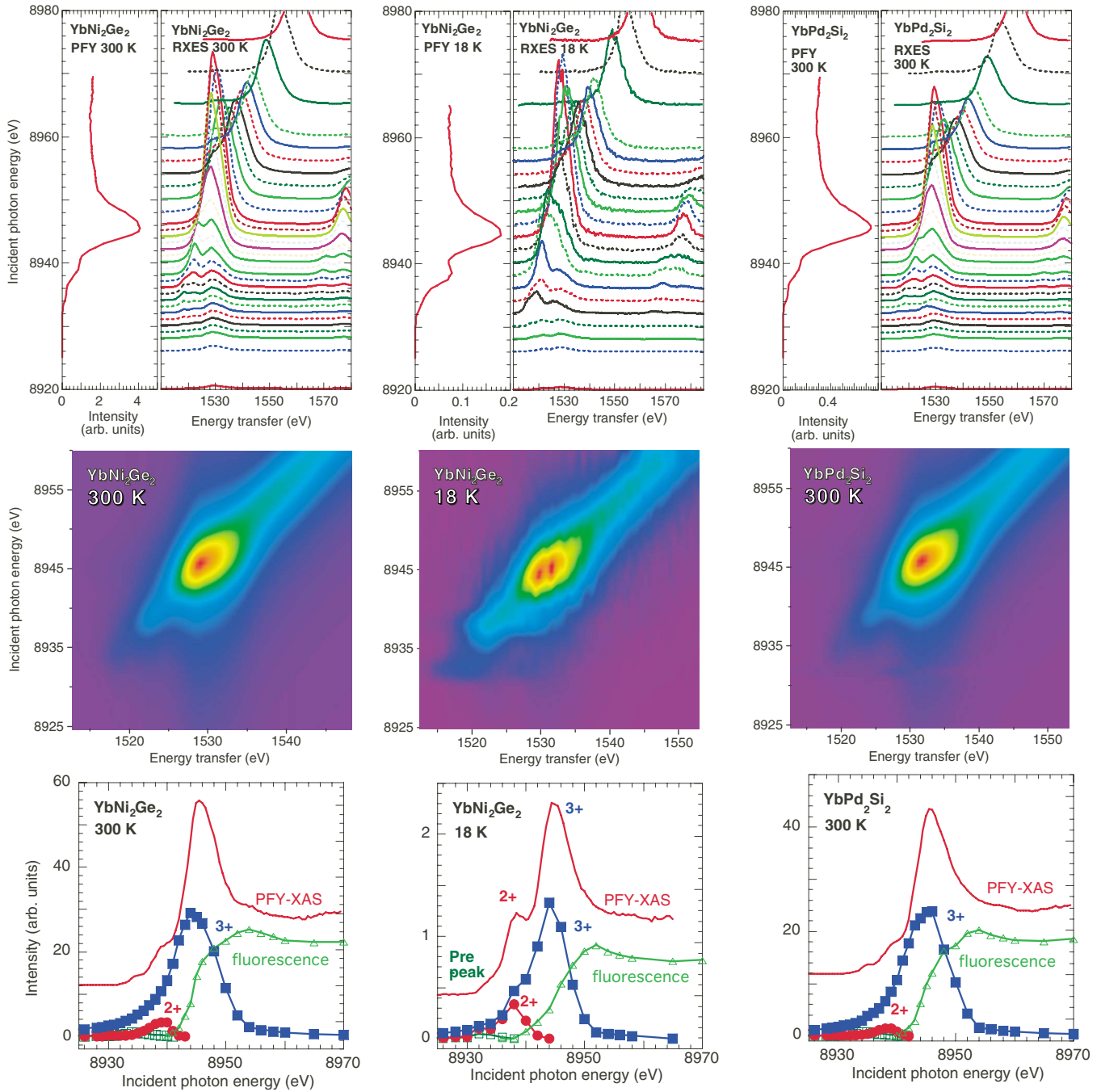
FIG. 4. (Color online) (Top panels) $2p3d$-RXES spectra as a function of the incident photon energies with the corresponding PFY-XAS spectrum for $YbNi_2Ge_2$ at 300 and 18 K and $YbPd_2Si_2$ at 300 K. (Middle panels) Contour images of the RXES spectra. (Bottom panels) Incident energy dependence of the intensity of 2+ and 3+ Raman and fluorescence components inferred from the fit of the RXES spectra.

which is a temperature scale below which the system enters the Fermi-liquid state, was shown by resistivity to rapidly decrease with increasing pressures and becomes zero at 5 GPa. As seen in Fig. 6(b), the coefficient A of the resistivity drastically increases around 4 GPa and ρ_0 is maximum around 7.5 GPa,[8] where the maximum of ρ_0 in the magnetic phase may coincide with the full ordering. These occurrences may seemingly correspond to the gradual transition around 5 GPa in our pressure dependence of the valence in Fig. 6(a).

IV. DISCUSSION

The Mössbauer spectra had been measured for $YbPd_2Si_2$ at 0, 4.3, and 5.4 GPa, in which pressure-induced change in the valence close to 3+ was observed at 4.3 GPa.[46] Recently Ovsyannikov *et al.*[18] reported a phase transition around 6 ± 0.5 GPa by measuring of thermoelectric and dilatometric properties. At 1 GPa, Nakano *et al.*[11] suggested the onset of magnetic ordering at 1 GPa below 0.5 K by resistivity, hinting at a QCP between 0 and 1 GPa while in $YbNi_2Ge_2$ the
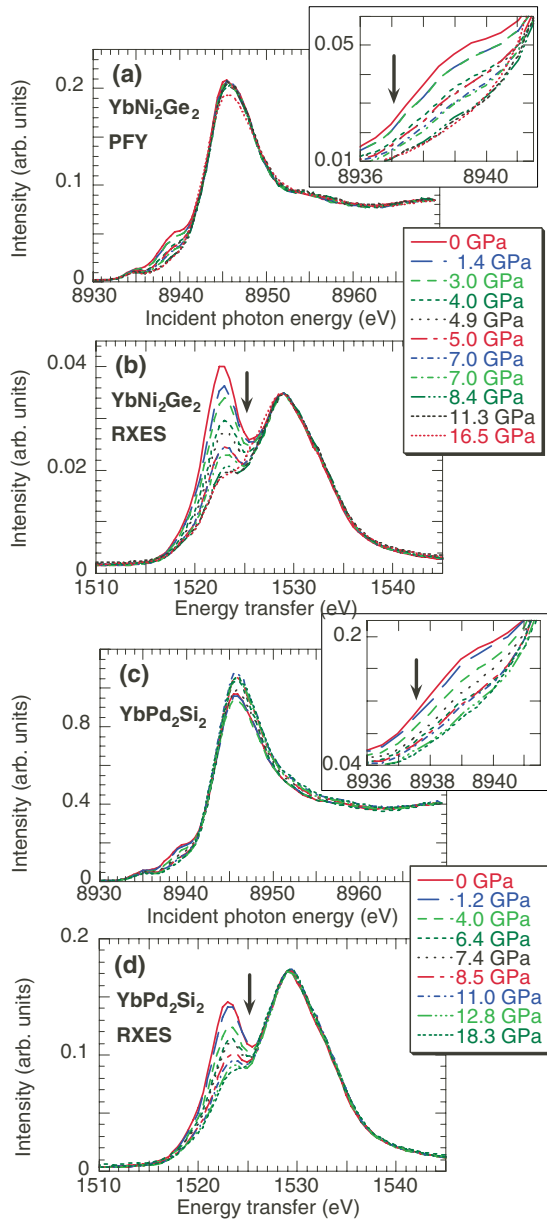
FIG. 5. (Color online) Pressure dependence of the Yb L_3 PFY-XAS and $2p3d$-RXES (E_{in}=8934 eV) spectra measured for YbNi$_2$Ge$_2$ and YbPd$_2$Si$_2$. The inset in each figure is the enlarged 2+ component and arrows in the figures indicate the intensity trend with decreasing temperature.

Kondo lattice exists to higher pressure around 4 GPa. They also reported on a resistivity minimum around 5–8 GPa, attributed to the interplay between magnetic ordering and single-ion Kondo effect. Our results agree well with these previous studies as the valence is found to change gradually mostly around 5–8 GPa, although we found weak pressure dependence on the valence in the 0–1 GPa range. The increase in the valence in YbPd$_2$Si$_2$ is slower than in YbNi$_2$Ge$_2$. This could be explained by the larger lattice constant of YbPd$_2$Si$_2$ compared with YbNi$_2$Ge$_2$ as shown in Table I.

It is important to note that the present results in YbNi$_2$Ge$_2$ reveal a pressure-induced transition from Fermi liquid to

magnetic ordered state through a QCP, accompanied by a slight change in the valence. The solid lines in Figs. 6(a) and 6(c) correspond to the fits using an arctanlike (asymmetrical double sigmoid) functions. The pressure points on curves, at which the second derivative change sign, are around 5.0 GPa for YbNi$_2$Ge$_2$ and 5.3 GPa for YbPd$_2$Si$_2$, respectively. This fact indicates again that around the QCP of YbNi$_2$Ge$_2$ the valence is not integer. Normally, the phase transition at the QCP is mainly described by two scenarios: the conventional spin-density-wave (SDW) QCP and the Kondo breakdown at the antiferromagnetic (AFM) QCP.[27] In the latter scenario, a breakdown of the Kondo screening occurs at the QCP, implying a transition to an integer valence state. This has been previously reported to account for the QCP of CeCu$_{6-x}$Au$_x$ (Ref. 27) and YbRh$_2$Si$_2$.[31] The fact that the valence of YbNi$_2$Ge$_2$ is noninteger at the QCP suggests that this scenario should be ruled out. Furthermore, from previously published resistivity data, no SDW seems to occur in YbNi$_2$Ge$_2$ which rules out the SDW interpretation too. This implies that another scenario should be considered to describe the QCP of YbNi$_2$Ge$_2$. Here we note that in YbAuCu$_4$ Wada *et al.*[30] discussed the competition between the valence and spin fluctuations in the vicinity of the QCP, where superconductivity appears. Theoretical considerations by Miyake group[28,29] indicate that the superconducting correlation is enhanced near the QCP by the coherent motion of the electrons with valence fluctuation, that is, cooper paring mediated by the valence fluctuation. Thus the valence-fluctuation phenomenon (noninteger valence) near the QCP is physically important, as it can relate to superconductivity too. A similar variation in valence was also observed in the chemical composition dependence of YbCu$_{5-x}$Al$_x$,[24] which could suggest that a slight valence transition is a common occurrence around the QCP. Pressure-dependent measurements of the valence at low temperature might reveal a more pronounced effect near the QCP.

Here we note the pressure effect on the degeneracy. Knebel *et al.* plotted (Fig. 8 of Ref. 8) the pressure variation in A and T^{max}, where T^{max} is the high- or low-temperature maximum in the magnetic contribution of the resistivity. The ratio $A/(T^{max})^2$ increases by a factor of 20–30 when the pressure is increased up to 4 GPa in YbNi$_2$Ge$_2$. This curve relates to the Kadowaki-Woods law: A/T_K^2=const, where T_K is Kondo temperature.[6,7] The change in the slope of the A $-T^{max}$ curve can correspond to a change in the degeneracy. At ambient pressure the valence fluctuation and the Kondo effect are dominant compared to the CEF effect and the theoretical curve assuming $J=7/2$ describes well the temperature dependence of the susceptibility for YbNi$_2$Ge$_2$ as shown in Fig. 1. At high pressure, the CEF effect gets stronger while the Kondo temperature decreases, and thus the degeneracy becomes smaller.

The resistivity measurements on Yb$_{1-x}$La$_x$Pd$_2$Si$_2$ showed that La substitution results in the expansion of the unit cell, corresponding to negative chemical pressure.[47] The transformation from Fermi liquid (Kondo lattice) to a single-ion Kondo effect region was observed as well as in the case applying external pressure,[11] and a decrease in the mean valence of observed by magnetic susceptibility. This confirms that negative chemical pressure and external pressure cause
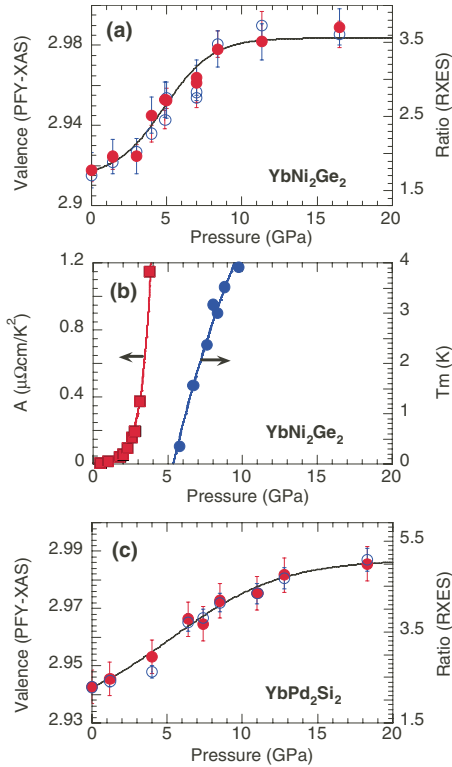
FIG. 6. (Color online) [(a) and (c)] Pressure dependence of the Yb valence (closed circles) derived from the PFY-XAS spectra. Open circles correspond to the intensity ratio of Yb^{2+} to Yb^{3+} derived from the RXES spectra at $E_{in} = 8934$ eV. Solid lines in (a) and (c) correspond to the fits for the valence derived from the PFY-XAS spectra. In (b) the A coefficient and T_m are shown for $YbNi_2Ge_2$ as a function of pressure. The data are taken from the Ref. 8.

opposite effects to the Yb valence in $YbPd_2Si_2$. Here we note that interestingly a similar pressure-induced resistivity minimum could be observable also in $YbNi_2Ge_2$.[8]

Opposite volume effect on the Kondo effect and RKKY interaction are indeed expected between Ce122 and Yb122 systems due to the electron-hole symmetry. By applying pressure, the Ce compounds go into an intermediate valence state which results in an increase in the Kondo temperature and a concomitant decrease in the Neel temperature. Conversely, in Yb compounds the Neel temperature increases with pressure. It is interesting to note that the critical behavior around the transition point is often different between these systems, abrupt, first order in the Ce case, and rather continuous for Yb. For example, in $CeRh_2Si_2$ the transition from AFM order to a paramagnetic (PM) state is believed to be first order with a volume discontinuity.[48] On the other hand, $YbRh_2Si_2$ shows a continuous change from AFM to PM under pressure.[49] This difference in the pressure dependence between these systems has been explained by two kinds of scenarios. One is the stronger localization of the $4f$ shell in Yb than in Ce and the other is the substantially stronger spin-orbit coupling of Yb than Ce.[48] Our present results are consistent with these observations, as they suggest that a slow crossover from Fermi liquid to magnetically ordered state occurs for both Yb compounds. The pressure dependence of the valence has not been reported yet for

$CeNi_2Ge_2$ and $CePd_2Si_2$, but we believe that the comparison with the Yb122 systems will be interesting because of the analogy with the relation between $CeRh_2Si_2$ and $YbRh_2Si_2$.

Here comparison of the pressure and temperature dependences may bring a comprehensive understanding of the Yb valence transitions. Upon both cooling and pressure increase lattice contraction occurs, although resulting in opposite changes in the valence. In Yb compounds and Yb metal the volume is normally decreased in the order of at least 10% with increasing the pressure up to $\sim$10 GPa.[50,51] This results in an increase in the Yb^{3+} ratio due to the smaller Yb^{3+} ion radius compared with Yb^{2+}, thus favoring the occurrence of magnetic ordering. Recently, a hole-doping mechanism for the closed $4f$ shell (Yb^{2+} state) with growing hybridization of the $4f$ band with the *spd* band has been put forward for the pressure-induced effects on the electronic structure of $4f$ systems.[52] Colarieti-Tosti *et al.*[53] also had proposed a related idea of the *d-f* pairing due to Coulomb attraction between the hole in the $4f$ shell and promoted $5d$ electrons (corresponding to Falikov interaction). On the other hand, the change in the volume upon cooling is normally much less than 1%,[54] so that the change in the valence cannot be explained by the Kondo volume collapse scenario. It is well described by the Anderson impurity model, which accounts for the screening of the magnetic moments subsequent to the growing $4f$-$5d$ hybridization, which leads to an increase in the charge fluctuations with decreasing the valence.

Finally, one can try to understand the temperature and pressure-induced valence-transition mechanisms qualitatively based on the energy scale of the temperature normalized by the Kondo temperature, T/T_K. Thus, T/T_K decreases with decreasing temperature, resulting in an increase in the Kondo effect and accordingly stronger valence fluctuations. On the other hand, as the pressure is increased at a given temperature, the Kondo temperature decreases while the valence increases.[55,56] This is confirmed in our case as the A coefficient of $YbNi_2Ge_2$ increases rapidly with pressure, corresponding to the strong decrease in T_K, hence the increase in T/T_K and eventually the suppression of valence fluctuations.

V. CONCLUSION

We have measured both temperature- and pressure-induced valence transitions for $YbNi_2Ge_2$ and $YbPd_2Si_2$ using bulk-sensitive x-ray spectroscopic probes. For both compounds the temperature dependence of the valence can be well described by the Anderson impurity model. The valence is found to closely follow χT throughout the measured temperature range. Our high-pressure results show second-order valence transitions toward trivalence for both compounds with $YbPd_2Si_2$ having a more gradual transition than $YbNi_2Ge_2$. The valences for both compounds are estimated to be slightly less than 3+ at ambient pressure so that small changes in the valence on the order of 0.03–0.05 are sufficient to drastically alter the magnetic and electronic properties. The pressure-induced valence transitions of $YbNi_2Ge_2$ are found to be correlated with the pressure dependence of the resistivity. Especially, an increase in the valence is observed to coincide with the QCP near 6 GPa whereas in

YbPd$_2$Si$_2$ no correlation was found between the pressure dependence of the valence and the presumed existence of a QCP near 1 GPa.

[1] Z. Ban and M. Sikirica, Acta Crystallogr. **18**, 594 (1965).

[2] F. Steglich, J. Aarts, C. D. Bredl, W. Lieke, D. Meschede, W. Franz, and H. Schäfer, Phys. Rev. Lett. **43**, 1892 (1979).

[3] P. Strange, A. Svane, W. M. Temmerman, Z. Szotek, and H. Winter, Nature (London) **399**, 756 (1999).

[4] C. N. R. Rao, D. D. Sarma, P. R. Sarode, E. V. Sampathkumaran, L. C. Gupta, and R. Vijayaraghavan, Chem. Phys. Lett. **76**, 413 (1980).

[5] S. L. Bud'ko, Z. Islam, T. A. Wiener, I. R. Fisher, A. H. Lacerda, and P. C. Canfield, J. Magn. Magn. Mater. **205**, 53 (1999).

[6] K. Kadowaki and S. B. Woods, Solid State Commun. **58**, 507 (1986).

[7] N. Tsujii, H. Kontani, and K. Yoshimura, Phys. Rev. Lett. **94**, 057201 (2005).

[8] G. Knebel, D. Braithwaite, G. Lapertot, P. C. Canfield, and J. Flouquet, J. Phys.: Condens. Matter **13**, 10935 (2001).

[9] S. K. Dhar, E. V. Sampathkumaran, and R. Vijayaraghavan, Solid State Commun. **61**, 479 (1987).

[10] P. Schlottmann, Phys. Rev. B **46**, 217 (1992).

[11] T. Nakano, M. Hedo, Y. Uwatoko, and E. V. Sampathkumaran, Solid State Commun. **132**, 325 (2004).

[12] E. V. Sampathkumaran, K. H. Frank, G. Kalkowski, G. Kaindl, M. Domke, and G. Wortmann, Phys. Rev. B **29**, 5702 (1984).

[13] P. Bonville, J. Hamann, J. A. Hodges, P. Imbert, G. Jéhanno, M. J. Besnus, and A. Meyer, Z. Phys. B: Condens. Matter **82**, 267 (1991).

[14] J. A. Hodges and G. Jéhanno, J. Phys. (Paris) **45**, 1663 (1984).

[15] P. Bonville and J. A. Hodges, J. Magn. Magn. Mater. **47-48**, 152 (1985).

[16] P. Bonville, J. A. Hodges, P. Imbert, D. Jaccard, J. Sierro, M. J. Besnus, and A. Meyer, Physica B **163**, 347 (1990).

[17] P. Bonville, J. Hamann, J. A. Hodges, P. Imbert, G. Jéhanno, D. Jaccard, M. J. Besnus, and A. Meyer, Physica B **171**, 171 (1991).

[18] S. V. Ovsyannikov, V. V. Shchennikov, T. Fujikawa, and Y. Uwatoko, J. Phys. Chem. Solids **69**, 2301 (2008).

[19] I. Jarrige, H. Ishii, Y. Q. Cai, J.-P. Rueff, C. Bonnelle, T. Matsumura, and S. R. Shieh, Phys. Rev. B **72**, 075122 (2005).

[20] H. Yamaoka, M. Taguchi, A. M. Vlaicu, H. Oohashi, Y. Yokoi, D. Horiguchi, T. Tochio, Y. Ito, K. Kawatsura, K. Yamamoto, A. Chainani, S. Shin, M. Shiga, and H. Wada, J. Phys. Soc. Jpn. **75**, 034702 (2006).

[21] H. Yamaoka, N. Tsujii, K. Yamamoto, H. Oohashi, A. M. Vlaicu, K. Kunitani, K. Uotani, D. Horiguchi, T. Tochio, Y. Ito, and S. Shin, Phys. Rev. B **76**, 075130 (2007).

[22] H. Yamaoka, H. Oohashi, I. Jarrige, T. Terashima, Y. Zou, H. Mizota, S. Sakakura, T. Tochio, Y. Ito, E. Ya. Sherman, and A. Kotani, Phys. Rev. B **77**, 045135 (2008).

[23] H. Yamaoka, N. Tsujii, K. Yamamoto, A. M. Vlaicu, H. Oohashi, H. Yoshikawa, T. Tochio, Y. Ito, A. Chainani, and S. Shin, Phys. Rev. B **78**, 045127 (2008).

[24] H. Yamaoka, I. Jarrige, N. Tsujii, N. Hiraoka, H. Ishii, and K.-D. Tsuei, Phys. Rev. B **80**, 035120 (2009).

[25] H. Yamaoka, H. Sugiyama, Y. Kubozono, A. Kotani, R. Nouchi, A. M. Vlaicu, H. Oohashi, T. Tochio, Y. Ito, and H. Yoshikawa, Phys. Rev. B **80**, 205403 (2009).

[26] I. Jarrige, J.-P. Rueff, S. R. Shieh, M. Taguchi, Y. Ohishi, T. Matsumura, C.-P. Wang, H. Ishii, N. Hiraoka, and Y. Q. Cai, Phys. Rev. Lett. **101**, 127401 (2008).

[27] A. Schröder, G. Aeppli, R. Coldea, M. Adams, O. Stockert, H. v. Löhneysen, E. Bucher, R. Ramazashvili, and P. Coleman, Nature (London) **407**, 351 (2000).

[28] A. T. Holmes, D. Jaccard, and K. Miyake, J. Phys. Soc. Jpn. **76**, 051002 (2007).

[29] K. Miyake, J. Phys.: Condens. Matter **19**, 125201 (2007).

[30] S. Wada, A. Yamamoto, K. Ishida, and J. L. Sarrao, J. Phys.: Condens. Matter **20**, 175201 (2008).

[31] S. Friedemann, T. Westerkamp, M. Brando, N. Oeschler, S. Wirth, P. Gegenwart, C. Krellner, C. Geibel, and F. Steglich, Nat. Phys. **5**, 465 (2009).

[32] B. Coqblin and J. R. Schriffer, Phys. Rev. **185**, 847 (1969).

[33] V. T. Rajan, Phys. Rev. Lett. **51**, 308 (1983).

[34] N. E. Bickers, D. L. Cox, and J. W. Wilkins, Phys. Rev. B **36**, 2036 (1987).

[35] G. Polatsek and P. Bonville, Z. Phys. B: Condens. Matter **88**, 189 (1992).

[36] H. Oesterreicher and F. T. Parker, Phys. Rev. B **16**, 5009 (1977).

[37] We note that as performed in Ref. 24, only $\Delta n_f(0)$ should be a free parameter in the fit, fixing $n_f(\infty)$ reduced from the conduction bandwidth D of La- or Lu-based nonmagnetic compounds. But unfortunately we could not find the reference sample data for YbNi$_2$Ge$_2$ and YbPd$_2$Si$_2$.

[38] J. M. Lawrence, P. S. Riseborough, C. H. Booth, J. L. Sarrao, J. D. Thompson, and R. Osborn, Phys. Rev. B **63**, 054427 (2001).

[39] A. N. Tahvildar-Zadeh, M. Jarrell, and J. K. Freericks, Phys. Rev. B **55**, R3332 (1997).

[40] A. L. Cornelius, J. M. Lawrence, T. Ebihara, P. S. Riseborough, C. H. Booth, M. F. Hundley, P. G. Pagliuso, J. L. Sarrao, J. D. Thompson, M. H. Jung, A. H. Lacerda, and G. H. Kwei, Phys. Rev. Lett. **88**, 117201 (2002).

[41] A. M. Umarji, C. Godart, L. C. Gupta, and R. Vijayaraghavan, J. Magn. Magn. Mater. **63-64**, 623 (1987).

[42] Y. Kishimoto and T. Ohno, Phys. Lett. A **317**, 308 (2003).

[43] J. L. Sarrao, C. D. Immer, Z. Fisk, C. H. Booth, E. Figueroa, J. M. Lawrence, R. Modler, A. L. Cornelius, M. F. Hundley, G. H. Kwei, J. D. Thompson, and F. Bridges, Phys. Rev. B **59**, 6855

(1999).

[44] M. N. Groshev, M. D. Koterlin, E. M. Levin, R. V. Lutsiv, N. M. Miftakhov, Yu P. Smirnov, A. E. Sovestnov, A. V. Tyunis, V. A. Shaburov, R. I. Yasnitskiǐ, S. M. Kuz'mina, V. I. Petrova, and V. A. Tyukavin, Sov. Phys. Solid State **28**, 1519 (1987).

[45] M. J. Besnus, M. Benakki, A. Braghta, H. Danan, G. Fischer, J. P. Kappler, A. Meyer, and P. Panissod, J. Magn. Magn. Mater. **76-77**, 471 (1988).

[46] J. Moser, K. H. Munch, and G. M. Kalvius, Hyperfine Interact. **40**, 405 (1988).

[47] I. Das, E. V. Sampathkumaran, and R. Vijayaraghavan, Physica B **186-188**, 485 (1993).

[48] R. Boursier, A. Villaume, G. Lapertot, D. Aoki, G. Knebel, and J. Flouquet, Physica B **726**, 254 (2008).

[49] J. Plessel, M. M. Abd-Elmeguid, J. P. Sanchez, G. Knebel, C. Geibel, O. Trovarelli, and F. Steglich, Phys. Rev. B **67**, 180403(R) (2003).

[50] H. Winkelmann, M. M. Abd-Elmeguid, H. Micklitz, J. P. Sanchez, P. Vulliet, K. Alami-Yadri, and D. Jaccard, Phys. Rev. B **60**, 3324 (1999).

[51] M. Hofmann, S. J. Campbell, P. Link, S. Fiddy, and I. Goncharenko, Physica B **385-386**, 330 (2006).

[52] E. R. Ylvisaker, J. Kuneš, A. K. McMahan, and W. E. Pickett, Phys. Rev. Lett. **102**, 246401 (2009).

[53] M. Colarieti-Tosti, M. I. Katsnelson, M. Mattesini, S. I. Simak, R. Ahuja, B. Johansson, C. Dallera, and O. Eriksson, Phys. Rev. Lett. **93**, 096403 (2004).

[54] A. L. Cornelius, J. M. Lawrence, J. L. Sarrao, Z. Fisk, M. F. Hundley, G. H. Kwei, J. D. Thompson, C. H. Booth, and F. Bridges, Phys. Rev. B **56**, 7993 (1997).

[55] M. V. Mushnikov, T. Goto, A. V. Kolomiets, K. Yoshimura, W. Zhang, and H. Kageyama, J. Phys.: Condens. Matter **16**, 2395 (2004).

[56] T. Goto, N. V. Mushnikov, K. Yoshimura, and W. Zhang, J. Magn. Magn. Mater. **272-276**, E25 (2004).